Available online at www.sciencedirect.com

SCIENCE DIRECT®

Quaternary International 131 (2005) 11–22

New $^{40}Ar/^{39}Ar$, stratigraphic and palaeoclimatic data on the Isernia La Pineta Lower Palaeolithic site, Molise, Italy

M. Coltorti[a,*], G. Feraud[b], A. Marzoli[c], C. Peretto[d], T. Ton-That[e], P. Voinchet[f], J.-J. Bahain[f], A. Minelli[d], U. Thun Hohenstein[d]

[a]Dipartimento di Scienze della Terra, Universita di Siena Via di Laterina 8, 53100 Siena, Italy
[b]CNRS, UMR 6526 Géosciences Azur, Université de Nice-Sophia Antipolis, Parc Valrose, 06108 NICE cedex 02, France
[c]Dipartimento di Mineralogia e Petrologia, Università di Padova, Corso Garibaldi 37, 35137, Padova, Italy
[d]Dipartimento di Scienze della Terra, Università di Ferrara, Corso Ercole I D'Este, 44100 Ferrara, Italy
[e]Département de Minéralogie, Université Genève, 13 rue des Maraîchers, 1211 Genève-4, Switzerland
[f]Laboratoire de Préhistoire du Muséum national d'Histoire naturelle, Institut de paléontologie humaine, UMR 6569 du CNRS, 1, rue René Panhard, 75013 Paris, France

Available online 28 October 2004

Abstract

The archaeological deposits of Isernia la Pineta are a milestone in the European context, being composed of very rich and large-sized occupation layers. The archaeological remains are characterised by the use of anvils in a very opportunistic and rapid way to produce a large number of flakes and residual cores, usually of very small size. The lithic instruments are associated with remains of large mammals, which give a clear indication of the diet. They are represented by *Bison schoetensacki* Freudenberg, *Stephanorhinus hundsheimensis* Toula, *Elephas (Palaeoloxodon) namadicus* Falconer e Cautley, *Ursus deningeri* von Reichenau, *Hippopotamus* cf. *antiquus* Desmarest, *Sus scrofa* L., *Hemitragus* cf. *bonali* Harlè e Stehlin, *Megaceroides solilhacus* Robert, *Cervus elaphus* cf. *acoronatus* Beninde, *Dama dama* cf. *clactoniana* Falconer, *Capreolus* sp., and *Panthera leo fossilis* von Reichenau.

The rodent fauna is represented by *Clethrionomys* sp., *Pliomys episcopalis* Mèhely, *Pliomys lenki* Heller, *Microtus* aff. *arvalis* Pallas, *Microtus brecciensis* Gieber, *Microtus* (*Terricola*) gr. *multiplex-subterraneus*, and *Arvicola cantiana* Hinton. The insectivores are *Talpa* sp., *Sorex* cf. *runtonensis* Hinton, and *Crocidura* sp.

Two main archaeological layers have been identified. The lower one (Sector I, layer 3C) rests on a phytoclastic travertine passing laterally to a phytohermal travertine, which generated a small step in the watercourse. A sandy silt layer of lacustrine environment (layer 3b) deposited inside travertine pools and very limited phytostromatolitic travertine sediments cover this layer. The second occupation layer (layer 3a) rests on these sediments as well as on the travertines. Cross-bedded fine gravelly sands cover the deposits and are interlayered with tuffs very rich in pyroxene and sanidine. The latter gave $^{40}Ar/^{39}Ar$ ages of 610 ± 10 and 606 ± 2 ka (2σ error). This layer is covered by cross-bedded gravels weathered by a thick Alfisols with a well-expressed Bt horizon. The uppermost part of the series is composed of gravels and colluvia containing another pyroclastic layer. Sanidines of this layer yield scattered Ar/Ar ages, with a main population at about 504 ± 14 ka. A maximum age of 474 ± 3 ka is inferred for this layer.

The Isernia travertines are not associated with hot water springs and indicate that the area was frequented at the end of an Interglacial period. The new ages demonstrate that the human frequentation occurred at the beginning of the Middle Pleistocene.

1. Introduction

The Isernia La Pineta site (Fig. 1a) is one of the earliest Italian archaeological sites (Coltorti et al., 1981, 1982; Cremaschi, 1983; Cremaschi and Peretto, 1988; Anconetani et al., 1992). The degree of preservation is unusual: flint and cherty limestone artefacts were found mixed with a very rich palaeontological assemblage. Moreover, the artefacts are found in more than one archaeological layer and all of them are enclosed in a very clear stratigraphic context. The stratigraphy of the

*Corresponding author. Tel.: +39-0577-298811.
E-mail address: coltorti@unisi.it (M. Coltorti).

1040-6182/$ - see front matter
doi:10.1016/j.quaint.2004.07.004

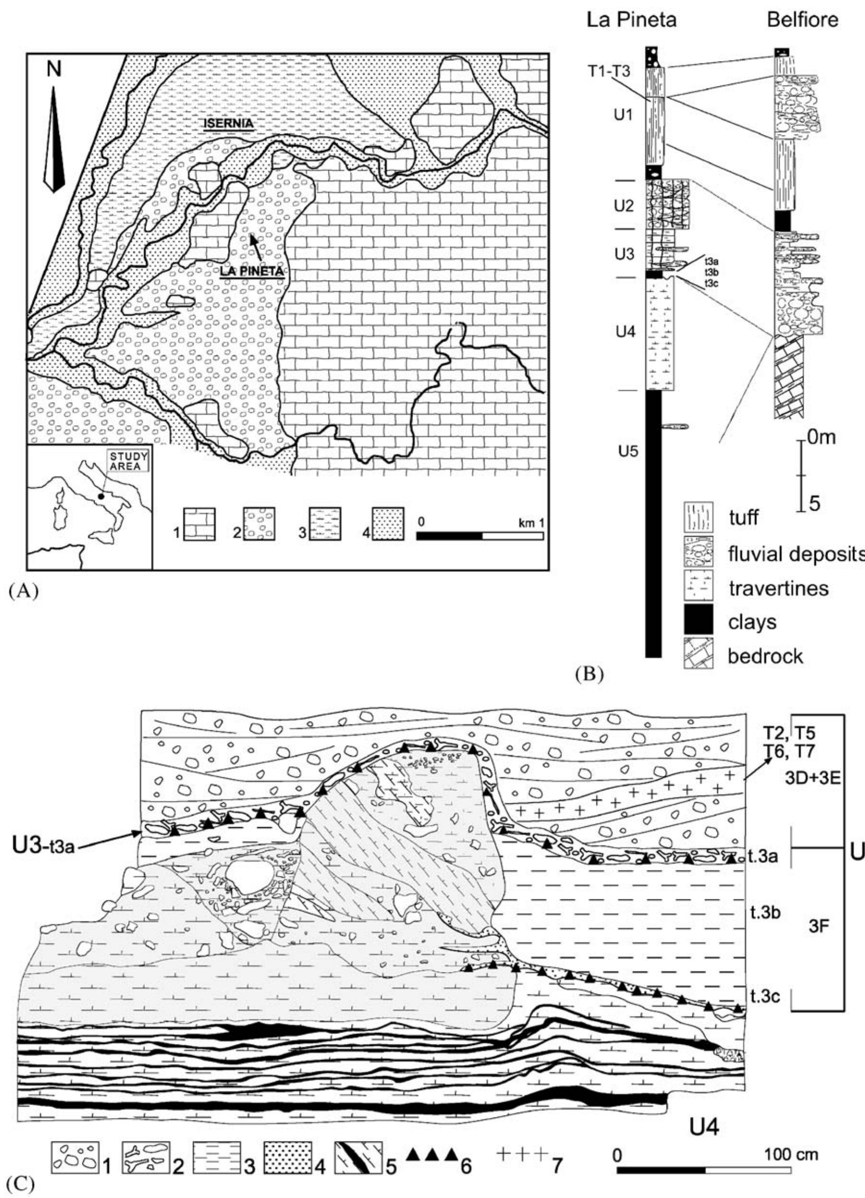

Fig. 1. Stratigraphic setting and location of the site. 1A: 1, limestone bedrock; 2, main filling of the basin; 3, travertines; 4, recent fluvial deposits; 1B: Stratigraphic sequence of Isernia La Pineta and Villa Belfiore with the indication of the lithological units utilised by Cremaschi (1993); 1C, detailed stratigraphy of Unit 3 in correspondence of the archaeological site: 1, archaeological horizons (t.3a); 2, clays (t.3b); 3, archaeological horizon, t.3c; 4, travertines with organic layers.

site (Fig. 1b and c) was described mostly by Coltorti and Cremaschi (1982) and by Cremaschi (1983), who recognised five main lithological units. The oldest palaeoethnological remains (Unit 3, t. 3c of Cremaschi, 1983) lie directly on the travertine and are covered by a clay layer. The main occupation level (Unit 3, t. 3a), lying on top of the clay layer as well as on the travertines, is revealed by the unusual concentration of flint and limestone artefacts associated with mammal remains that mostly consist of large bones and reworked blocks of travertine in a sandy matrix. Many pyroclastic layers are present in the sequence. The older one, composed of up to 10–20 cm thick of reworked and well sorted elements including large crystals of sanidine (analysed by the Ar/Ar method), and pyroxene, lies on top of the main occupation layer (Unit 3, t.3a also indicated as u.3E). The younger ones, composed of up to 3 superimposed layers of fall deposits, each one 20–30 cm thick, including pumice, sanidine pyroxene and large biotite crystals, are located inside the upper alluvial and colluvial complex, usually within the profile of the uppermost palaeosol (Unit 1, layers 1B, 1C, 1D). These uppermost tephras, located a few metres below the ground surface, are widespread across the area.

The occupation layers were previously dated by means of the K/Ar method and also by palaeomagnetic investigations which were carried out within the series. The K/Ar method was applied to the three uppermost tephras as well as to the pyroclastic material overlying the main occupation layer. Inside Unit 1, Delitala et al. (1983) dated two pyroclastic layers at 470 ± 50 and 550 ± 50 ka, respectively. Sevink et al. (1981), in a nearby locality, dated a pyroclastic layer supposed to be coeval to the previously mentioned ones at 730 ± 50 ka. However, at least the former two ages are not consistent with those of the pyroclastic materials located on top of the archaeological horizon which gave an age of 730 ± 40 ka (1σ uncertainty) (Coltorti et al., 1982; Delitala et al., 1983). The palaeomagnetic investigations revealed that the magnetic polarity underwent a major change from negative in the part of the section below the first occupation layers, to positive in the layers overlying the occupation layer. The presence of coarse debris in the upper part of the sequence prevented more investigations.

The chronological setting of Isernia was used to calibrate other Italian archaeological or palaeontological sites because the rich assemblage of fauna was very peculiar (Sala, 1983; Gliozzi et al., 1999). The assemblage is represented by *Bison schoetensacki* Freudenberg, *Stephanorhinus hundsheimensis* Toula, *Elephas (Palaeoloxodon) namadicus* Falconer e Cautley, *Ursus deningeri* von Reichenau, *Hippopotamus* cf. *antiquus* Desmarest, *Sus scrofa* L., *Hemitragus* cf. *bonali* Harlè e Stehlin, *Megaceroides solilhacus* Robert, *Cervus elaphus* cf. *acoronatus* Beninde, *Dama dama* cf. *clactoniana* Falconer, *Capreolus* sp., and *Panthera leo fossilis* von Reichenau. The rodent fauna is represented by *Clethrionomys* sp., *Pliomys episcopalis* Mèhely, *Pliomys lenki* Heller, *Microtus* aff. *arvalis* Pallas, *Microtus brecciensis* Gieber, and *Microtus (Terricola)* gr. *multiplex-subterraneus*, *Arvicola cantiana* Hinton. The insectivores are *Talpa* sp., *Sorex* cf. *runtonensis* Hinton, and *Crocidura* sp. This assemblage suggests the presence of a wooded environment at least on the valley floor surrounded by more open areas.

Polmonate shell remains were discovered inside silty and clayey layers below the travertine (Esu, 1983). They are represented by *Lymnaea truncatula* (Muller), *Vertigo pygmaea* (Draparnaud), *Vertigo moulinsiana* (Dupuy), *Pupilla muscorum* (Linnaeus), *Vallonia pulchella* (Muller) and *Succinea oblonga* (Drapanaud). These species are not extinct and are commonly associated with the cold phases of the Lower and Middle Pleistocene deposits of Europe.

More recently, due to the chronological setting of similar mammal assemblages in northern Europe, the chronological setting of the Isernia site was criticised and some authors suggested a younger age (van Kolfschoten, 1998; Roebroeks and van Kolfschoten, 1998). It is therefore crucial to perform precise dating experiments that can furnish unambiguous ages of the fossils. We have chosen to undertake $^{40}Ar/^{39}Ar$ laser analyses on single grains or small clusters of sanidine in order to constrain the age of the tuff layers that bracket the archaeological strata. This approach, including some step heating experiments, permits recognition of xenocrystic components (with older apparent ages) or secondary alteration (with younger apparent ages). Moreover, the statistical distribution of ages of a large number of analyses on single sanidine crystals gives a good indication of the primary or reworked nature of the deposit. Ar/Ar ages obtained on different mineral separates issued from distinct sampling, and performed in two different laboratories (Geneva and Nice), adopting different techniques (total fusion and step-heating) are identical, within analytical errors. New stratigraphic investigations were also carried out in the archaeological site.

2. Geological and geomorphological setting

The site of Isernia is located at the periphery of the town with the same name along the Velturno River basin and in particular along the valley of the Cavaliere-Sordo River not far from the watershed. The site, which is located at an elevation of about 400 m a.s.l., lies inside the main filling of the basin. It represents the oldest and morphostratigrapically highest sedimentological unit described in the basin. This unit was cut by the subsequent deepening of the valley. The downcutting was interrupted and fluvial terraces of limited extent were deposited at progressive heights on the valley floor. However, there is no agreement on the number of terraces and their age is poorly constrained (Coltorti, 1983; Van Otterloo and Sevink, 1983; Brancaccio et al., 1997).

The basin is bordered by a series of NE–SW and NW–SE-oriented faults with major fault escarpments arranged in a series of steps. Minor horsts and grabens with the same orientation are found in the lower part of the basin. These extensional faults displace the Apennine Platform Units which tectonically overlie the Sannitic, the Molisan and the Apulian Units in the northern part of the basin (Corrado et al., 1997; Di Bucci et al., 1999). These units were deposited since the Mesozoic, in marine basins characterised by different types of sedimentation and evolution, and were affected by eastward tectonic movements during the Messinian-Lower Pliocene. However, the normal faults not only displace these units but also the remains of a planation surface which levelled all the previous structural units as well as previous topographic contrasts created during the contractional phase (Coltorti and Cremaschi, 1982; Coltorti, 1983). Thousands of metres of erosion are locally ascertained considering the thickness of the original series missing on top of the structural units of the chain. Calamita et al. (1999) and Coltorti and Pieruccini (1999, 2002) suggest that this planation surface corresponds to a plain of marine erosion, and the latter authors, on the basis of general considerations on the stratigraphic relationship all along the Apennine chain, claim a possible Late Lower Pliocene age for the end of its evolution in the axial part of the Apennine chain, including the Isernia area. Little information is available on the chronostratigraphic setting of this "planation surface" for the Isernia area. Here, the planation occurred after the Messinian (age of the younger planated terrain) and before deposition of the oldest sediments inside the tectonic depressions. However, west of the basin, in the Campobasso area, Middle Pliocene marine sediments are also planated and suggest that planations occurred also in younger times in the Peri-Adriatic domain (Coltorti and Pieruccini, 2002).

The onset of the extensional tectonics in the basin also is poorly constrained due to the limited informations on the age of the sediments which fill the deeper part of the Upper Volturno basin. They have been attributed mostly to the Middle Pleistocene and only for a limited thickness to the Lower Pleistocene (Coltorti et al., 1982; Brancaccio et al., 1997).

3. Stratigraphy

The stratigraphy of the main filling was established by Coltorti and Cremaschi (1982) and Cremaschi (1983). From the bottom to the top the sequence is represented by: Unit 5, lacustrine clays with thin layers of gravels and debris (maximum thickness 70 m); Unit 4, travertines (maximum thickness, 50 m); Unit 3, palustrine deposits with sands and fine gravels; Unit 2, sands and gravels; Unit 1, gravels and sands with intercalated tuffs. In the nearby Villa Belfiore Section a thicker alluvial unit is interlayered inside Unit 1. According to Cremaschi (1983) palaeosoils are preserved at: (a) the base of the sequence (S4); (b) the top of the travertines (S3); (c) the top of the alluvial units (S2); and (d) the top of the sequence (S1). Therefore, Cremaschi established four main lithostratigraphic units that could be connected to four climatic cycles. Archaeological remains have been collected in two sectors located SW (Sector I) and NE (Sector II) of the railway line. These layers are found inside the lithostratigraphic Unit 3F (Fig. 1) which is subdivided into three layers, the uppermost and lowermost (t.3a and 3c) containing the palaeoethnological remains while the intermediate one (t.3b) is sterile. New stratigraphic and sedimentological investigations are ongoing on these deposits in the Isernia basin and we report the observations made in correspondence to the archaeological layers (Fig. 1C).

The travertines are constituted by interlayering of different facies: (1) phytoclastic travertine sands; (2) phytostromatic travertines; (3) phytohermal travertines; and (4) silt and clay lacustrine deposits following the classification made by Golubic et al. (1993) which has genetic significance. Facies 1 is composed of sands derived from the fluvial reworking of Facies 2 and 3. Facies 2 is associated with stromatolite (algal) deposition occurring in a thin vein of water, as along waterfalls; it is for this reason that the laminae can be very steep and this is also a diagnostic property for palaeoenvironmental reconstructions. Facies 3 is associated with incrustations along small obstacles such as blocks, and alive and dead vegetation which is preserved in places inside the travertine. The progressive precipitation of carbonates in coincidence with steps and obstacles could generate small lakes and ponds that could host the lacustrine deposition of Facies 4.

In the Isernia site all four travertine facies have been recognised, but the thin alternation of phytoclastic travertine sands and lacustrine deposits indicate that, at least in the studied section the ponds were very shallow and lasted for a short time. According to the recent investigations in the archaeological area, a phytohermal origin is established for the uppermost travertines below the archaeological remains (Unit 3, t.3.c). These are lying on phytoclastic travertine alternated with thin layers of silty sediments. Some of these layers are associated with phytostromatolitic travertine generated along small waterfalls. These layers have sets dipping 30–40° to the NE. It was very surprising to find that these sediments sealed few bones and flint artefacts belonging to layer 3C. Clay sediments of layer 3F (t.3b) can be interpreted as associated to the growth of a travertine ridge which dammed the river flow. Therefore, from a lithostratigraphic point of view, they should be included in the travertine Unit 4. Unit 3 would begin with the main occupation layer (t.3a) lying unconformably on the travertine as well as on the clay horizon (t.3b). It is remarkable that the two archaeological layers, most probably deposited very close in time, record two different depositional environments.

Actually travertine deposition (when not linked to hot water springs) occurs along water courses characterised by high CO_2 concentration, very low solid load and almost constant discharge as documented in many areas of Europe. Travertine is commonly associated with karst areas because the underground drainage reduces the solid load and generates a more constant flow. These dynamics were widespread in Italy (Cilla et al., 1996) as well as in most parts of Europe (Goudie et al., 1993; Viles et al., 1993) during the Early Holocene when most of the solid load was blocked on the slopes by the dense vegetation which was also responsible for the high concentration of CO_2 in the underground waters. Similar conditions, and therefore similar processes, were established in previous Interglacials suggesting that the human frequentation of the lowermost horizon (t.3c) at Isernia occurred at the end of a major Interglacial.

The reason for the declining of travertine sedimentation during the Holocene has been associated with the progressive deforestation of European (Viles et al., 1993) as well as of the Italian woodlands (Cilla et al., 1996). In the Lower and Middle Pleistocene, this process was climatically driven and therefore it is suggested that the main archaeological horizon (t.3a) at Isernia was associated with the onset of a cold period.

Lithostratigraphic Unit 3D, is made up of gravels, coarse sands and finer sediments in the upper part. The structures are mostly trough cross-bedded sands and gravels (Gt and St of the classification of Miall, 1985, 1996) and only locally there are horizontally laminated sands and gravels (Sh and Gh). Laterally and/or upward coarse trough cross-bedded and/or horizontally bedded gravels can be intercalated with fine sediments (Fm). These association of facies witness the presence of a braided river with very flat sandy and gravelly bars similar to the one observed in arid environments (Miall, 1996). In Italy similar facies characterised the river dynamics during the cold Stadial phases of the last Glaciation even at very low elevations (Calderoni et al., 1991; Coltorti and Dramis, 1995).

These observations confirm the existence of a very important change in the regime of the water course most probably associated to a drastic climatic change, from a forested landscape during an Interglacial to a very cold phase of a cold and arid Stadial. However, the correspondence of these stages with the deep sea core stratigraphy is still uncertain from a stratigraphic point of view. Recent investigations also pointed out that the transition from travertine to gravels and sands is not marked by the presence of a palaeosol (S3) as suggested by Cremaschi (1983). Locally, the top of the travertines is weathered by a very deep soil, mostly characterised by a reddish Bt horizon. However, this horizon has also weathered the overlying gravels and it is therefore subsequent to these, being associated with the S2 soil. The weathering front is wedge-shaped and therefore its depth changes considerably from place to place. The severe leaching of the gravels inside the wedge is documented by the composition of the alluvial sediments constituted only by cherts, quartz and siliceous gravels. This suggests the complete dissolution of more than 70% of the volume (the composition of the unweathered gravels rarely contains more than 30% flint). When these wedges reach the travertine, the result is even more dramatic because the dissolution can result in a volume reduction of more than 90%, leaving only the reddish clayey fraction. As a consequence, a series of depressions are generated which affected the overlying alluvial sediments. In correspondence to these depressions the fauna is not preserved, whereas the limestone artefacts (chopper and chopping tools) are absent in any archaeological layer due to their complete weathering. Luckily, the wedge configuration of the weathered front preserved a large part of the settlement where all the original components can be studied. Most probably, the very scarce preservation of fauna in Sector II, mostly constituted by ivory teeth, is because the weathering front affected most of the deposits.

In summary, within the upper part of the sequence, deep weathered palaeosols occur only at the top of the sequence of the main filling and on top of the alluvial sequence (Units 1 and 2). These palaeosols are surely related to long lasting Interglacials. Most probably, the uppermost unit evolved during the Holocene because it has been observed above more recent geomorphological units (i.e. terraces) and sometimes it contains pottery fragments and other archaeological remains (Van Otterloo and Sevink, 1983).

The volcanic materials located in different layers have a varying significance and composition. The uppermost volcanic layer found within Unit 1 (Fig. 1B) has a homogeneous thickness across a long distance, although locally it fills wide depressions that resemble palaeochannels. In correspondence to these depressions, colluviation has been observed, leading to local reworking of these materials. However, reworking was very limited, and samples were collected where reworking was absent.

The lowermost layer is very thick in places (up to 60 cm), and displays a wedge-like shape, representing the infilling of small channels. Laterally, this layer becomes progressively thinner, and in correspondence to some parts of the main occupation layer (t.3a), it is preserved only as small pockets. However, the homogeneous composition of the sediments suggests that, although the layer was affected by reworking processes, these occurred over very short distances and almost simultaneously with the volcanic event. Reworking over slightly longer distances should have led to the incorporation of allochthonous material (i.e. limestones).

4. $^{40}Ar/^{39}Ar$ geochronology

4.1. Analytical methods, Geneva

The analysed tephra layers are Unit 1, layer 3C, and Unit 3, layer 3E Isernia La Pineta, The largest and best preserved sanidine grains (315–500 μm fraction) were accurately selected and separated. The crystals were packed in copper disks along with multiple samples of the neutron fluence monitor mineral Alder Creek sanidine (1.19 Ma; Renne et al., 1998) and irradiated for 30 min in the TRIGA reactor, using the Cadmium-Lined In-Core Irradiation Tube (CLICLIT) facility at

Oregon State University, receiving fast neutron doses of $\sim 4.5 \times 10^{16}$ n/cm^2.

The sanidine grains were loaded in a copper planchette in one to five grains per well. After a short predegassing step at 10% laser power, gas was extracted with an infrared continuous laser. Detailed analytical and technical procedures at the University of Geneva are described in Ton–That et al. (2001). System blanks were run for every two samples analysed and were typically 0.5–1 order of magnitude smaller than the samples ($^{40}Ar \sim 10^{-17}$ moles), and between 25% and 75% of the signal ($^{36}Ar \sim 10^{-19}$ mol.). The mass discrimination was monitored with an on-line air pipette and was 1.0034 ± 0.0008 per amu. Corrections for neutron-induced reactions on ^{40}K and ^{40}Ca are: $[^{40}Ar/^{39}Ar]_K = 0.00086$; $[^{36}Ar/^{37}Ar]_{Ca} = 0.000264$; $[^{39}Ar/^{37}Ar]_{Ca} = 0.000673$.

The total fusion measurements of the samples are reported in relative probability density diagrams (ideograms, Deino and Potts, 1990), except for gas samples that were below detection limits. These were not included in the calculations, either. As the analyses were performed on a population of one to five grains, the results that gave too young or too old ages were interpreted as a possible post-magmatic alteration or xenocrystic, respectively, and thus were not included in the calculation of the inverse isochron age.

The three different ages that are discussed later (total fusion, weighted mean and inverse isochron) overlap each other. The inverse isochron age is considered the most statistically reliable (York, 1969) and is preferred.

4.2. Analytical methods, Nice

The $^{40}Ar/^{39}Ar$ analyses were performed on single grains of about 600–1300 μm size. They were irradiated for 1 h in the nuclear reactor at McMaster University in Hamilton, Canada, in position 5c, within cadmium shielding. The total neutron flux density during irradiation is 1.3×10^{17} n cm^{-2}, with a maximum flux gradient estimated at $\pm 0.2\%$ in the volume where the samples were included. We used Fish Canyon sanidine (28.02 Ma; Renne et al., 1998) as monitor flux.

The gas extraction was carried out by a 50 W Synrad infrared continuous laser and the mass spectrometer was a VG 3600 working with a Daly detector system. The typical blank values of the extraction and purification laser system were in the range 80–140, 1–7, $2\text{–}4 \times 10^{-14}$ cm^3 STP for the mass 40, 39, 36, respectively, measured every third step, whereas argon isotopes measured on the sanidine single grains for total fusion experiments were on the order of 100–500 and 1000–20,000 times the blank level, for the ^{40}Ar and ^{39}Ar, respectively. In some cases, the ^{36}Ar was indistinguishable from the blank value. Corrections for neutron-induced reactions on ^{40}K and ^{40}Ca are: $[^{40}Ar/^{39}Ar]_K = 0.001$; $[^{36}Ar/^{37}Ar]_{Ca} = 0.000279$; $[^{39}Ar/^{37}Ar]_{Ca} = 0.000706$. K decay constants are those of Steiger and Jäger (1977).

5. Results

5.1. Unit 3, layer 3E

Twenty-eight total fusion analyses were obtained at Geneva, ranging in age from 451.2 ± 162.3 to 979.9 ± 35.2 ka (mean total fusion age of 622.0 ± 10.6 ka; 2σ analytical uncertainty; Table 1). They show a symmetrical distribution with a well-defined main probability maximum at 609.8 ± 9.8 ka on the ideogram (Fig. 2). All the analysed mineral aliquots have a moderate to high K/Ca (calculated from $^{37}Ar/^{39}Ar$), characteristic of alkali-feldspars (anorthoclase or sanidine). Anorthoclase and sanidine yield undistinguishable results. Twenty-six of the 28 subsamples form an inverse isochron age of 613.2 ± 11.2 ka, with a MSWD of 1.28 and a $^{40}Ar/^{36}Ar$ intercept of 280.4 ± 27.0, indistinguishable from the atmospheric ratio (Fig. 2b).

Four different samples from Unit 3, layer 3E (issued from a distinct sampling) were analysed in Nice with the step-heating and total-fusion method (after a predegassing step) on single grains (Tables 2 and 3; Fig. 3). They are T2 (18 grains in total, only 8 grains are shown on Fig. 3), and T5, T6, T7 (4 grains each). The data are generally concordant, 15 fusion step ages vary from 587 ± 20 to 628 ± 22 ka (2σ uncertainties). The weighted mean ages calculated on fusion steps are 606 ± 2, 599 ± 12, 606 ± 9 and 601 ± 10, for samples T2, T5, T6 and T7, respectively. Two concordant plateau ages of 614 ± 14 and 606 ± 10 ka were measured on two single grains from T2, whereas another plateau age from T2 is significantly older (637 ± 13 ka), and its age spectrum is characterised by decreasing ages at increasing temperatures. Therefore, these four samples probably belong to the same formation that was deposited very early after the eruption(s) (from which the analysed sanidines originated). Calculation from all fusion steps and the two concordant plateau ages (discarding the 637 ka plateau age), gives a weighted mean age of 606 ± 2 ka for Unit 3, layer 3E. The homogeneity (and purity) of the sanidine population in these four samples is confirmed by the $^{37}Ar_{Ca}/^{39}Ar_K$ ratio measured on fusion steps that is mostly clustered between 0.009 and 0.011. Plotting the data (excluding the predegassing steps that may correspond to alteration phases) on an inverse isochron (not shown) shows that most are closely clustered, because of the low atmospheric contamination, and therefore no useful information can be deduced. The age is 604 ± 4 ka (concordant with the weighted mean age).

Table 1
$^{40}Ar/^{39}Ar$ data for 28 individual total fusion analyses of Isernia La Pineta tephra feldspar, Unit 3, layer 3E

Sample	# Grains	% Laser power	$^{40}Ar/^{39}Ar$	$^{37}Ar/^{39}Ar$	$^{36}Ar/^{39}Ar$	$^{40}Ar^*$ (10^{-16} mol)	% $^{40}Ar^*$	K/Ca	Apparent age (ka) $\pm 2\sigma$	Used in isochron
GE15D32C	1	75	3.16396	0.00656	0.000205	3.27519	98.07	74.72	708.9±105.6	
GE15D32D	1	75	2.83664	0.00814	0.000203	3.20003	97.88	60.18	633.9±78.6	*
GE15D32F	1	75	4.71695	0.00890	0.006596	5.03350	58.67	55.04	632.1±59.7	*
GE15D32G	1	75	3.15538	0.04223	0.002579	1.83266	75.92	11.60	547.6±102.0	*
GE15D32H	2	75	3.20468	0.01130	0.002254	3.48726	79.22	43.37	580.1±70.3	*
GE15D32I	2	75	3.42413	0.01038	0.002792	7.86207	75.91	47.21	593.8±29.0	*
GE15D32J	2	75	4.26036	0.01519	0.006138	5.67964	57.43	32.25	559.2±61.2	*
GE15D32K	2	75	2.78180	0.12879	0.000601	4.98290	93.94	3.80	596.9±70.0	*
GE15D32L	2	75	3.94373	0.21357	0.003569	1.50956	73.66	2.29	663.8±269.5	*
GE15D32M	2	75	2.80517	0.01079	0.001408	3.82622	85.17	45.40	546.0±49.8	*
GE15D32N	2	75	3.70663	0.13775	0.004007	4.22704	68.32	3.56	578.7±44.4	*
GE15D32O	1	75	2.68376	0.01012	0.000302	4.54301	96.67	48.42	592.7±55.0	*
GE15D32P	2	75	3.07460	0.88654	0.003959	0.98719	64.17	0.55	451.2±162.3	*
GE15D32Q	2	75	3.04586	0.52505	0.001366	2.36822	88.06	0.93	644.9±93.2	*
GE15D32S	3	75	3.25327	0.46243	0.001705	3.92914	85.60	1.06	636.1±82.0	*
GE15D32T	3	75	2.81204	0.10010	0.000272	9.08855	97.39	4.89	625.9±23.2	*
GE15D32U	3	75	3.09080	0.30800	0.001306	5.23803	88.27	1.59	623.6±45.9	*
GE15D32V	3	75	3.00366	0.08886	0.002384	2.24796	76.75	5.51	526.6±70.8	*
GE15D32W	4	75	2.74993	0.01039	0.000223	17.84230	97.61	47.16	613.3±12.5	*
GE15D32X	4	75	2.79537	0.01304	0.000309	11.91660	96.74	37.58	618.0±19.9	*
GE15D32Z	4	75	2.90890	0.01103	0.000916	8.82813	90.69	44.43	602.8±36.7	*
GE15D320	4	75	2.87400	0.01032	0.000855	11.02183	91.21	47.50	599.1±35.4	*
GE15D321	4	75	2.97875	0.01038	0.001095	10.32776	89.14	47.22	606.8±24.6	*
GE15D322	4	75	7.11814	0.00836	0.009567	10.95520	60.28	58.64	979.9±35.2	
GE15D323	4	75	3.27840	0.00883	0.002001	5.80552	81.96	55.52	614.0±48.9	*
GE15D324	4	75	2.99945	0.00857	0.000981	9.27648	90.33	57.17	619.1±20.8	*
GE15D325	4	75	3.21423	0.01746	0.001464	5.29597	86.56	28.06	635.8±45.8	*
GE15D327	1	75	3.01931	0.01495	0.001059	4.27965	89.64	32.77	618.7±82.9	*

Weighted mean age = 609.8±9.8 ka, MSWD = 1.29; Inverse isochron age = 613.2±11.2 ka, MSWD = 1.28, $^{40}Ar/^{36}Ar$ intercept = 280.4±27.0; Total fusion age = 622.0±10.6 ka; $J = 0.0001257$.

The initial $^{40}Ar/^{36}Ar$ ratio is poorly defined but nearly atmospheric (318±20, MSWD = 1.3).

The total-fusion and step-heating $^{40}Ar/^{39}Ar$ ages obtained in the two laboratories are indistinguishable, within error, and are substantially younger and more precise than the K–Ar age of 730±40 ka (1σ; Coltorti et al., 1982). The high homogeneity of ages obtained on 58 single grains of sanidine of different sizes and from different samplings demonstrates that these investigated layers are not, or only slightly, reworked. This is in good agreement with the observation that reworking of the volcanic deposit was almost simultaneous with tephra fall. Consequently, this age probably corresponds to the emplacement of these layers and therefore to the fossil deposits.

5.2. Unit 1, layer 3C

Total-fusion ages of 23 feldspars, analysed at Geneva (Table 4; Fig. 4) display a relatively scattered age distribution, with a main distribution peak at 498.5±11.3 ka. The 23 analyses range from 206.4±189.2 to 599.1±32.4 ka (average age of 501.0±12.0 ka). All the analysed mineral aggregates have K/Ca characteristic of anorthoclase or sanidine. Twenty subsamples yield an inverse isochron age of 503.7±13.8 ka, with a $^{40}Ar/^{36}Ar$ intercept of 282.0±23.3, not different from air and a MSWD = 1.13.

Step-heating analyses of sanidine single grains from samples T1 and T3 of the same layer (performed in Nice; Tables 2, 3; Fig. 5) displayed discordant ages, ranging from 468±20 to 539±6 ka for T1 (4 grains) and from 456±28 to 555±8 ka for T3 (4 grains). One precise plateau age of 474±3 ka could be calculated on seven steps of one single grain from the T1 sample (Fig. 5).

These data, and particularly the step-heating analyses, show that the Unit 1, layer 3c is clearly reworked and is composed of heterogeneous populations of sanidine originating probably from distinct volcanic eruptions. The age of the deposit (probably younger than 474±3 ka) cannot be deduced from these results. Notably, a similar conclusion is consistent with scattered K/Ar ages for the same formation (470±50 and 550±50 ka, Coltorti et al., 1982).

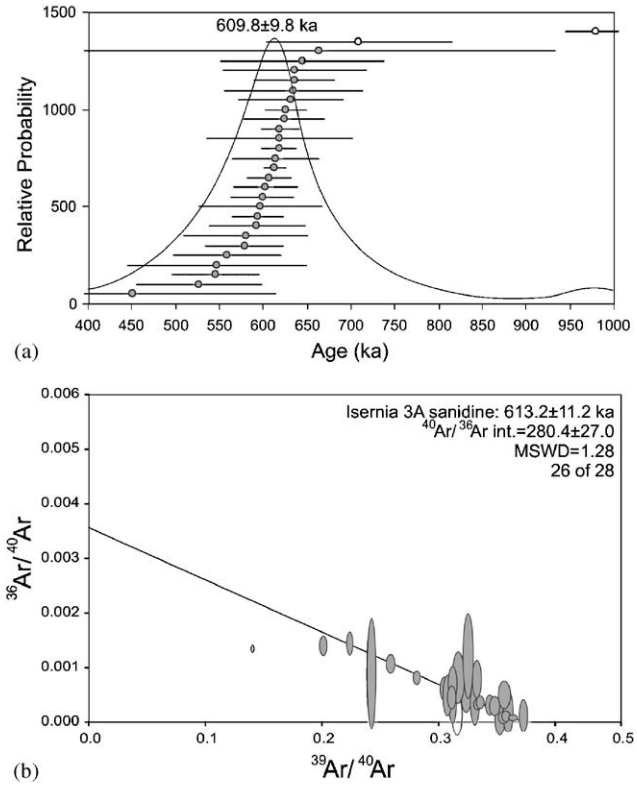

Fig. 2. Results of sanidine total fusion $^{40}Ar/^{39}Ar$ analyses of Unit 3, layer 3E. (a) Probability density plot (ideogram) of apparent total-fusion ages (ka = thousands year before present). Filled symbols represent analyses included in the inverse isochron calculations. (b) Inverse isochron diagrams of $^{40}Ar/^{39}Ar$ feldspar analyses. The filled ellipses are analyses included in the regression calculation, open ellipses are omitted from calculation. Mean standard weighted deviation (MSWD) and $^{40}Ar/^{36}Ar$ intercept values are reported. 2σ uncertainties are shown.

Table 2
$^{40}Ar/^{39}Ar$ ages of step-heating analyses on single grains of Isernia La Pineta tephra feldspar, Unit 3, layer 3E (T2, T5, T6 and T7); Unit 1 (T1 and T3)

Sample	Fusion step age (ka) ±2σ	Plateau age (ka) ±2σ	Weighted mean (ka) ±2σ	Weighted mean (ka) ±2σ
		637±13		
		614±14		
		606±10		
T2	618±10			
	598±18			
	604±40			
	600±14			
	591±16		606±2	
	616±10			
	596±14			
	619±14			
	611±8			
	601±6			
	602±6			606±2
	615±18			
	617±8			
	609±8			
	602±4			
	600±22			
T5	595±32		599±12	
	617±24			
	587±20			
	628±22			
T6	607±22		606±9	
	604±18			
	596±16			
	604±28			
T7	602±18		601±10	
	600±20			
	601±16			
	504±6			
T1		474±6		
	468±20			
	539±6			
	548±24			
T3	484±22			
	555±8			
	456±28			

The weighted mean age calculated on the four samples T2, T5, T6 and T7 (lower formation) excluded the discordant plateau age at 637 ± 13 Ma.

6. Conclusions

The new stratigraphic investigations constrain the facies and significance of the Isernia sequence which contains archaeological remains. The two archaeological layers of Sector I are associated with a major change in the environmental dynamics. The occupation of Unit 3, layer 3c, occurred during the last phases of the travertine deposition during an Interglacial period when the slopes were covered by thick woodland vegetation. Some flint tools are buried not only by lacustrine clays but also by phytohermal travertine. Unit 3, layer 3a, was deposited at the top of the travertine layers and was covered by alluvial sediments deposited in an arid (and most probably cold) environment. Fluvial facies associated with a high surcharge of solid load in the riverbed and high seasonality of precipitation is common. The human occupation occurred therefore at the beginning of a Glacial stage. No leached horizons have been observed in between these layers, as suggested by Cremaschi (1983). The reddish wedge-shaped argillic horizons observed in places, are the result of the deep weathering coming from palaeosoil S2, located on top of Unit 2.

The detailed $^{40}Ar/^{39}Ar$ data give much better constraints on the age of this archeological site than the previous K–Ar data. Unit 3, layer 3E contains yields indistinguishable $^{40}Ar/^{39}Ar$ ages on a large set of analysed sanidines (indicating that these minerals are

Table 3
Ar/Ar step-heating data on single grains for Isernia La Pineta, (a) Unit 3, layer 3E; (b) Unit 1

Laser power	Atmosph. contamin. (%)	^{39}Ar (%)	$^{37}Ar/^{39}Ar$	$^{40}Ar/^{39}Ar$	Apparent age (ka) $\pm 1\sigma$
(a) Unit 3, layer 3E					
T2					
212	51.300	1.37	0.027	1.078	485±217
264	17.223	3.20	0.024	1.249	563±102
311	8.510	9.77	0.022	1.441	649±27
350	13.270	29.22	0.022	1.438	648±14
Fuse	39.497	56.45	0.021	1.396	629±7
224	8.986	2.98	0.037	1.536	692±187
321	0.000	18.60	0.019	1.385	624±15
387	0.000	28.45	0.016	1.356	610±15
Fuse	0.000	49.96	0.016	1.360	612±8
218	0.000	1.40	0.039	1.816	818±159
306	12.092	4.79	0.032	1.307	589±41
348	4.301	21.30	0.028	1.352	609±14
379	0.000	12.12	0.029	1.356	611±24
Fuse	0.354	60.39	0.028	1.341	604±3
166	12.028	4.56	0.014	1.510	680±74
218	8.408	7.71	0.011	1.311	590±49
Fuse	25.597	87.74	0.010	1.372	618±5
238	67.853	6.15	0.019	1.340	603±136
Fuse	2.602	93.85	0.011	1.328	598±9
206	11.770	6.67	0.006	1.390	626±237
Fuse	3.167	93.33	0.011	1.341	604±20
237	2.905	3.61	0.021	1.509	680±226
Fuse	2.805	96.39	0.015	1.332	600±7
201	1.114	6.61	0.012	1.479	666±167
Fuse	3.694	93.39	0.011	1.312	591±8
227	0.000	0.16	0.007	2.316	1043±287
Fuse	1.011	5.75	0.010	1.369	616±6
226	41.596	0.22	0.022	0.917	413±186
Fuse	3.178	7.05	0.012	1.324	596±8
232	0.000	0.25	0.051	1.612	726±227
Fuse	0.324	7.90	0.010	1.376	620±7
230	0.000	0.35	0.000	1.628	733±192
Fuse	5.200	14.34	0.009	1.357	611±4
276	0.000	0.46	0.008	1.676	755±118
Fuse	2.348	10.83	0.010	1.337	602±3
236	9.849	0.43	0.022	1.432	645±66
Fuse	2.781	11.18	0.011	1.338	603±3
231	0.000	0.30	0.010	1.512	681±160
Fuse	0.478	5.72	0.011	1.366	615±9
264	0.000	0.28	0.006	1.764	794±125
Fuse	4.497	9.02	0.010	1.370	617±5
248	0.000	0.33	0.009	1.496	673±111
Fuse	0.227	7.69	0.009	1.354	610±4
259	6.322	0.48	0.012	1.792	807±74
Fuse	1.459	17.27	0.011	1.337	602±2
T5					
228	5.263	7.16	0.008	1.365	614±81
Fuse	3.485	92.84	0.010	1.332	600±11
202	55.547	6.35	0.016	0.690	311±184
Fuse	2.463	93.65	0.009	1.321	595±16
225	20.312	10.53	0.032	1.240	559±113
Fuse	2.758	89.47	0.013	1.371	617±12
209	43.401	7.79	0.021	0.857	386±96
Fuse	8.512	92.21	0.010	1.303	587±10

Table 3 (*continued*)

Laser power	Atmosph. contamin. (%)	^{39}Ar (%)	$^{37}Ar/^{39}Ar$	$^{40}Ar/^{39}Ar$	Apparent age (ka) $\pm 1\sigma$
T6					
204	0.000	2.32	0.000	2.843	1280±556
Fuse	2.373	97.68	0.012	1.395	628±11
196	0.000	2.54	0.009	1.920	865±412
Fuse	0.455	97.46	0.014	1.348	607±11
205	0.000	4.16	0.025	1.710	770±174
Fuse	55.397	95.84	0.010	1.342	604±9
219	7.885	6.88	0.008	1.511	680±86
Fuse	2.466	93.12	0.009	1.323	596±8
T7					
206	0.000	4.67	0.018	1.608	724±243
Fuse	4.401	95.33	0.013	1.341	604±14
246	37.917	3.04	0.014	1.042	469±255
Fuse	0.000	96.96	0.013	1.336	602±9
202	0.000	2.58	0.018	1.770	797±371
Fuse	9.659	97.42	0.012	1.333	600±10
199	42.320	3.36	0.012	0.938	422±225
Fuse	1.245	96.64	0.011	1.334	601±8
(b) Unit 1					
T1					
222	19.677	3.24	0.030	1.067	481±96
Fuse	1.193	96.76	0.023	1.120	504±3
321	5.086	2.54	0.029	1.154	520±29
410	2.606	2.85	0.018	1.062	478±14
501	2.729	5.72	0.017	1.036	467±9
550	28.810	21.68	0.016	1.059	477±4
570	0.904	37.60	0.016	1.054	475±2
589	0.000	18.65	0.016	1.060	477±3
640	1.927	8.39	0.016	1.039	468±6
Fuse	7.747	2.57	0.017	1.022	460±21
189	17.880	6.74	0.029	1.039	468±109
255	11.010	13.56	0.017	0.960	432±60
Fuse	5.136	79.71	0.018	1.039	468±10
207	0.000	1.81	0.014	1.717	773±97
318	8.957	11.86	0.014	1.198	539±19
Fuse	2.514	86.32	0.014	1.198	539±3
T3					
211	6.515	6.99	0.023	1.594	718±87
257	4.593	22.31	0.021	1.170	527±30
Fuse	0.541	70.70	0.020	1.216	548±12
273	34.740	9.40	0.038	0.855	385±90
Fuse	0.000	90.60	0.029	1.076	484±11
205	10.890	2.90	0.063	1.287	580±134
257	5.187	4.29	0.032	1.178	530±86
Fuse	0.409	92.81	0.026	1.233	555±4
250	40.064	11.52	0.051	0.715	322±78
Fuse	7.539	88.48	0.035	1.013	456±14

not, or only slightly, reworked), dated at 610±10 and 606±2 ka (in two laboratories) that probably represent the age of the anthropological layers of Isernia. Scattered sanidine ages for Unit 1, layer 3C suggest that this layer was partially reworked. The ages of the youngest sanidines suggest that its maximum age is 474±3 ka.

There is an apparent discrepancy between the geochronological data, that indicate that the anthropic occupation occurred at the beginning of the Middle Pleistocene, and the stratigraphic data that allow recognition of only two depositional cycles. However, this could be explained by the presence of major unconformities that led to the erosion of the sediments. The base of Unit 2, made of gravel, unconformably lies over the archaeological layers and the travertines. The base of Unit 2, made of gravel, unconformably lies over the archaeological layers and the travertines. The second unconformity is located at the base of Unit 1, on top of the palaeosols that developed over the alluvial sequence, and locally affect the entire gravel layer down to the travertine bedrock.

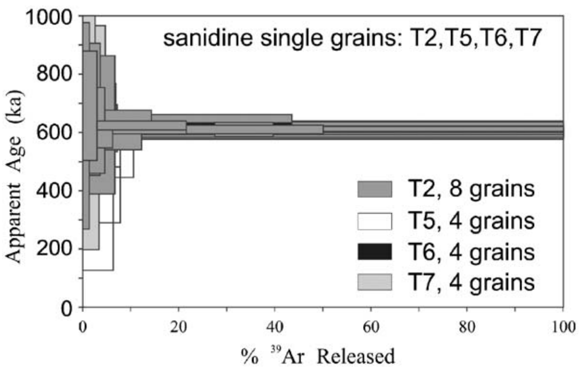

Fig. 3. $^{40}Ar/^{39}Ar$ age spectra on sanidine single grains from samples T2, T5, T6 and T7 belonging to Unit 3, layer 3E. For T2, only eight single grains among 18 are represented. Boxes on age spectra represent 1σ error bars.

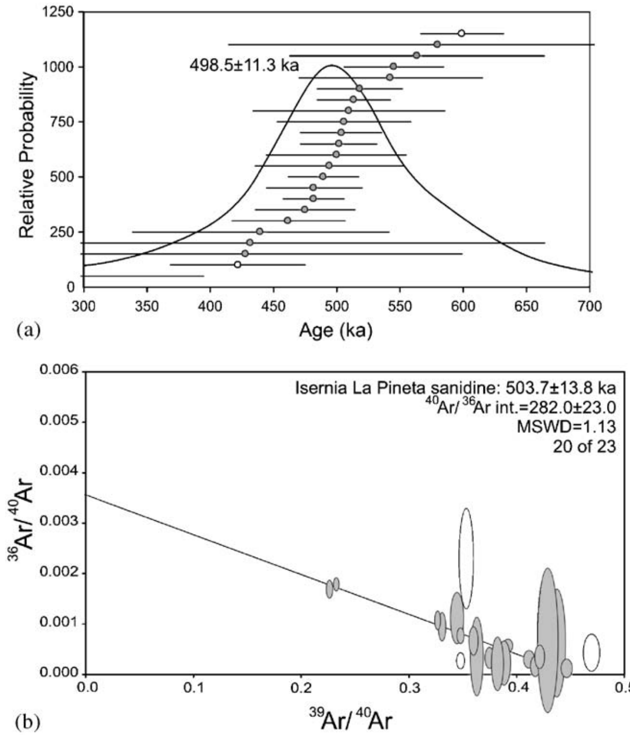

Fig. 4. results of sanidine total fusion $^{40}Ar/^{39}Ar$ analyses of Unit 1, layer 3C. (a) Probability density plot (ideogram) of apparent total-fusion ages. Filled symbols represent analyses included in the inverse isochron calculations. (b) Inverse isochron diagrams of $^{40}Ar/^{39}Ar$ feldspar analyses. The filled ellipses are analyses included in the regression calculation, open ellipses are omitted from calculation. 2σ uncertainties are shown.

Table 4
$^{40}Ar/^{39}Ar$ data for 23 individual total fusion analyses of Isernia La Pineta tephra feldspar, Unit 1

Sample	# Grains	% Laser power	$^{40}Ar/^{39}Ar$	$^{37}Ar/^{39}Ar$	$^{36}Ar/^{39}Ar$	$^{40}Ar^*$ (10^{-16} mol)	% $^{40}Ar^*$	K/Ca	Apparent age (ka) ±2σ	Used in isochron
GE15D31A	1	75	2.61570	0.00392	0.002772	0.53543	68.66	0.00	431.5±232.7	*
GE15D31B	1	75	2.13032	0.01111	0.000918	3.07675	87.27	44.10	421.7±53.2	
GE15D31D	1	75	2.82784	0.02910	0.006500	0.37501	32.13	16.38	206.4±189.2	
GE15D31E	1	75	2.29089	0.01514	0.000150	4.69566	98.08	32.37	509.5±75.6	*
GE15D31F	1	75	2.28738	0.01739	0.001354	1.50848	82.53	25.18	428.0±171.2	*
GE15D31G	1	75	2.75816	0.02233	0.000684	2.37210	92.70	21.94	579.4±164.5	*
GE15D31K	2	75	3.02457	0.01370	0.002850	4.45973	72.16	35.76	494.5±58.7	*
GE15D31L	2	75	2.57819	0.01425	0.000619	4.06811	92.91	34.38	542.8±73.0	*
GE15D31M	2	75	2.61825	0.01339	0.000449	2.92694	94.94	36.59	563.4±101.1	*
GE15D31N	3	75	2.87540	0.01577	0.002218	5.66409	77.22	31.08	503.4±32.0	*
GE15D31O	2	75	2.87695	0.01278	0.000792	6.76019	91.87	38.34	599.1±32.4	
GE15D31P	4	75	2.43057	0.10235	0.000765	5.61022	91.00	4.79	501.6±30.4	*
GE15D31Q	4	75	2.66957	0.06827	0.000913	7.09120	90.06	7.18	545.1±39.4	*
GE15D31R	3	75	4.42266	0.04271	0.007521	4.44913	49.80	11.47	499.6±55.6	*
GE15D31S	4	75	2.56628	0.01525	0.001022	6.90107	88.25	32.13	513.5±29.0	*
GE15D31T	4	75	2.56238	0.01163	0.001434	7.96913	83.46	42.12	481.8±24.0	*
GE15D31U	4	75	2.39813	0.01609	0.000382	6.42779	95.31	30.45	518.1±33.9	*
GE15D31V	4	75	2.78061	0.01137	0.001857	4.45082	80.26	43.10	506.0±52.9	*
GE15D31W	4	75	2.24036	0.02273	0.000280	5.87009	96.34	21.56	489.5±28.1	*
GE15D31X	4	75	2.37438	0.40395	0.000952	5.38370	89.44	1.21	481.8±38.0	*
GE15D31Y	4	75	4.30319	0.01429	0.007677	5.19506	47.00	0.29	461.6±44.7	*
GE15D31Z	4	75	3.06471	0.01979	0.003282	5.25665	68.37	24.76	475.1±39.8	*
GE15D310	4	75	2.90285	0.00000	0.003255	1.81899	66.80	0.00	439.8±101.3	*

Weighted mean age = 498.5±11.3 ka, MSWD = 1.15; Inverse isochron age = 503.7±13.8 ka, MSWD = 1.13, $^{40}Ar/^{36}Ar$ intercept = 282.0±23.3; Total fusion age = 501.0±12.0 ka; $l_B = 4.692 \times 10^{-10}$/yr; $J = 0.0001252$.

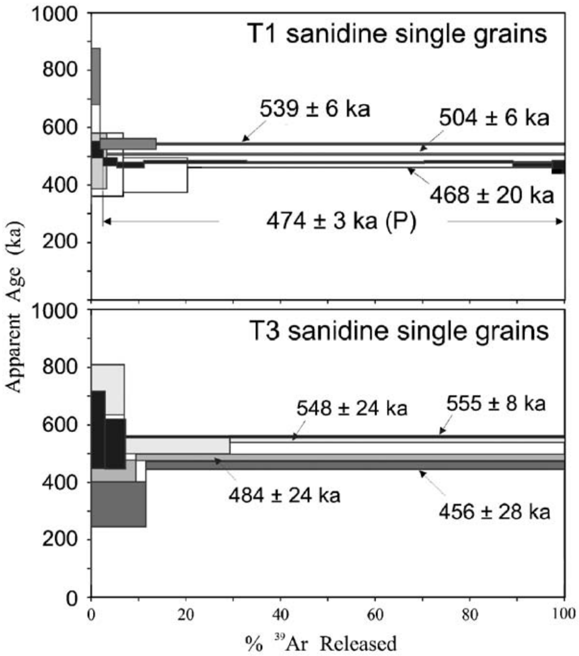

Fig. 5. $^{40}Ar/^{39}Ar$ age spectra on sanidine single grains from samples T1 and T3 belonging to Unit 1, layer 3C. (P) indicates plateau age. Error bars on ages are indicated at the 2σ level, whereas the boxes on age spectra represent 1σ error bars.

Acknowledgements

This is Contribution UMR Gépsciences Azur nb 580; CNR 2000, Siena Research unit coordinated by M. Coltorti. Cofin 2000, Ferrara Reseatrch Unit coordinated by C. Peretto, Soprintendenza per I Beni Archeologici del Molise, Programma Europeo TMR Progetto "Early Prehistoric Migrations", CNR Progetto Finalizzato Beni Culturali. The sampling of the levels dated in Nice was performed by J.-J. Bahain and P. Voinchet.

References

Anconetani, P., Crovetto, C., Ferrari, M., Giusberti, G., Longo, L., Peretto, C., Vianello, F., 1992. Nuove ricerche nel giacimento di Isernia La Pineta (Molise). Riv. Scienze Preist. XLIV, f.1–2.

Brancaccio, L., Cinque, A., Di Crescenzo, G., Santangelo, N., Scarciglia, F., 1997. Alcune osservazioni sulla tettonica quaternaria nell'alta valle del Fiume Volturno (Molise). Il Quaternario 10 (2), 321–328.

Calamita, F., Coltorti, M., Pieruccini, P., Pizzi, A., 1999. Evoluzione strutturale e morfogenesi Plio-Quaternaria dell'Appennino Umbro-Marchigiano tra il Pedappennino Umbro e la costa Adriatica. Bollittino Societa Geologica Italiana 118, 125–139.

Calderoni, G., Coltorti, M., Dramis, F., Magnatti, M., Cilla, G., 1991. Sedimentazione fluviale e variazioni climatiche nell'alto bacino dell'Esino durante il Pleistocene superiore. In: Tazioli, S. (Ed.), Fenomeni di erosione e alluvionamento degli alvei fluviali. University of Ancona, Ancona, pp. 171–190.

Cilla, M., Coltorti, M., Farabollini, P., Dramis, F., Gentili, B., Pambianchi, G., 1996. Fluvial sedimentation in the Early Holocene in the Marchean Valley (Central Italy). I1 Quaternario 9 (2), 459–464.

Coltorti, M., 1983. Le fasi principali dell'evoluzione del paesaggio nel bacino di Isernia (Molise). In: Coltorti, M. (Ed.), Isernia La Pineta, un accampamento più antico di 700.000 anni. Calderini, Bologna, pp. 41–47.

Coltorti, M., Cremaschi, M., 1982. Depositi quaternari e movimenti neotettonici nella conca di Isernia. Contributi Conclusivi per la carta Neotettonica d'Italia, Consiglio Nazionale Richerche. Progresso Fin. Geodinamica 506, 173–198.

Coltorti, M., Dramis, F., 1995. The chronology of Upper Pleistocene stratified slope-waste deposits in Central Italy. Permafrost and Periglacial Processes 6, 235–242.

Coltorti, M., Pieruccini, P., 1999. A Late Lower Pliocene planation surface across the Italian Peninsula: a key tool in neotectonic studies. Journal of Geodynamics, 1–6.

Coltorti, M., Pieruccini, P., 2002. The Late Lower Pliocene planation surface and mountain building of the Apennines (Italy), In: Dramis, F., Farabollini, P., Molin, P. (Eds.), Large-scale vertical movements and related processes. Studi Geologica Camerti, N.S., 1, 45–60.

Coltorti, M., Cremaschi, M., Delitala, M.C., Esu, D., Fornaseri, M., McPherron, A., Nicoletti, M., Van Otterloo, R., Peretto, C., Sala, B., Schmidt, V., and Sevink, J., 1981. Isernia La Pineta: lower paleolithic with fauna before 0.7 M.Y. In The Upper Volturno Basin, Central Italy: first report. X Congress Union of International Stratigraphic Paleontologists and Palynologists, Mexico 1981, 19-24/10/81, 58–63, Città del Messico.

Coltorti, M., Cremaschi, M., Delitala, M.C., Esu, D., Fornaseri, M., McPherron, A., Nicoletti, M., Van Otterloo, R., Peretto, C., Sala, P., Schmidt, V., Sevink, J., 1982. Reversed magnetic polarity at Isernia La Pineta, a new lower Paleolithic site in Central Italy. Nature 300, 173–176.

Corrado, S., Di Bucci, D., Leschiutta, I., Naso, G., Trigari, A., 1997. La tettonica quaternaria della Piana di Isernia nell'evoluzione strutturale del settore molisano. Il Quaternario 10 (2), 609–614.

Cremaschi, M., 1983. La serie pleistocenica di Isernia La Pineta (Molise) e la posizione stratigrafica dei suoli di abitato paleolitici in essa inclusi. In: Coltorti, M. (Ed.), Isernia La Pineta. Un accampamento più antico di 700.000 anni. Calderini, Bologna, pp. 49–62.

Cremaschi, M., Peretto, C., 1988. Les sols d'habitat du site paleolithique d'Isernia La Pineta (Molise, Italie). L'Anthropologie 92 (2), 643–682.

Deino, A., Potts, R., 1990. Single-crystal $^{40}Ar/^{39}Ar$ dating of the Olorgesailie formation, Southern Kenya Rift. Journal of Geophysical Research 95, 8453–8470.

Delitala, M.C., Fornaseri, M., Nicoletti, M., 1983. Datazioni Argon-Potassio sulla serie pleistocenica di Isernia la Pineta. In: Coltorti, T. (Ed.), Isernia La Pineta. Un accampamento più antico di 700.000 anni. Calderini, Bologna, pp. 65–66.

Di Bucci, D., Corrado, S., Naso, G., Parotto, M., Praturlon, A., 1999. Evoluzione tettonica neogenico-quaternaria dell'area molisana. Bollittino Societa Geologica Italiana 118, 13–30.

Esu, D., 1983. Malacofaune continentali della serie "La Pineta" Isernia. In: Coltorti, T. (Ed.), Isernia La Pineta.Un accampamento più antico di 700.000 anni. Calderini, Bologna, pp. 5–39.

Gliozzi, E., Abbazzi, L., Argenti, P., Azzarioli, A., Caloi, L., Capasso Barbato, L., Di Stefano, G., Esu, D., Girotti, O., Kotsakis, T., Masini, F., Mazza, P., Mezzabotta, C., Palombo, M.R., Petronio, C., Rook, L., Sala, B., Sardella, R., Zanalda, E., Torre, D., 1999. Biochronology of selected mammals, molluscs and ostracods from the Middle Pliocene to the Late Pleistocene in Italy. The State of the Art. Riv.Italiana Paleontologia e Stratigrafia 103 (3), 369–388.

Golubic, S., Violante, C., Ferreri, V., D'Argenio, B., 1993. Algal control and early diagenesis in Quaternary travertine formation (Rocchetta a Volturno, Central Apennines). Bollittino Societa Paleontologica Italiana 1, 231–247.

Goudie, A.S., Viles, H.A., Pentecost, A., 1993. The late Holocene Tufa decline in Europe. The Holocene 3, 181–186.

Miall, A.D., 1985. Architectural-element analysis: a new method of facies analysis applied to fluvial deposits. Earth Science Reviews 22, 261–308.

Miall, A.D., 1996. Geology of Fluvial Deposits. Springer, Berlin, pp. 582.

Renne, P.R., Swisher, C.C., Deino, A.L., Karner, D.B., Owens, T.L., DePaolo, D.J., 1998. Intercalibration of standards, absolute ages and uncertainties in $^{40}Ar/^{39}Ar$ dating. Chemical Geology 145, 117–152.

Roebroeks, W., van Kolfschoten, T., 1998. The earliest occupation of Europe: a view from the North. In: Aguirre, E. (Ed.), Atapuerca y la Evolucion Humana. Fundacion Ramon Areces, Madrid, pp. 153–168.

Sala, B., 1983. La fauna del giacimento di Isernia La Pineta. In: Coltori, T. (Ed.), Isernia La Pineta. Un accampamento più antico di 700.000 anni. Calderini, Bologna, pp. 71–79.

Sevink, J., Hebeda, E.H., Priem, H.N.A., Verschure, R.H., 1981. A note on an approximately 730.000 years old mammal fauna and associated human activities near Isernia, Central Italy. Journal of Archeological Science 8, 105–106.

Steiger, R.H., Jäger, E., 1977. Subcommission on geochronology: convention on the use of decay constants in geo and cosmochronology. Earth and Planetary Science Letters 36, 359–362.

Ton-That, T., Singer, B., Paterne, M., 2001. $^{40}Ar/^{39}Ar$ dating of Latest Pleistocene (41 ka) marine tephra in the Mediterranean Sea: implications for global climate records. Earth and Planetary Science Letters 84, 645–658.

van Kolfschoten, Th., 1998. Evidencia bioestratigrágica de la primers occupación de europa/Biostratigrafical evidence of the earliest occupation of Europe. In: Carbonell, E., Bermúdez de Castro, J.M., Arsuaga, J.L., Rodríguez, X. P. (Eds.), Los primeros pobladores de Europa: Ültimos descubrimientos y debate actual/ The First Europeans: Recent Discoveries and Current Debate. pp. 99–116.

Van Otterloo, R., Sevink, J., 1983. The Quaternary evolution of the Upper Volturno basin. In: Coltorti, T. (Ed.), Isernia La Pineta. Un accampamento più antico di 700.000 anni. Calderini, Bologna, pp. 35–39.

Viles, H.A., Burger, D., and Goudie, A., 1993. A reason for declining tufa deposition in Germany and Britain. Abstracts, 3rd International Conference on Geomorphology, Hamilton, Ontario. 49.

York, D., 1969. Least squares fitting of a straight line with correlated errors. Earth and Planetary Science Letters 5, 320–324.